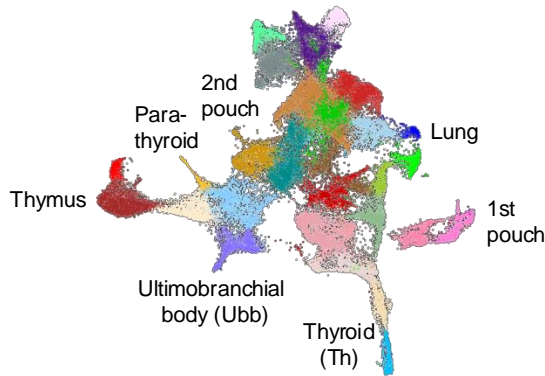
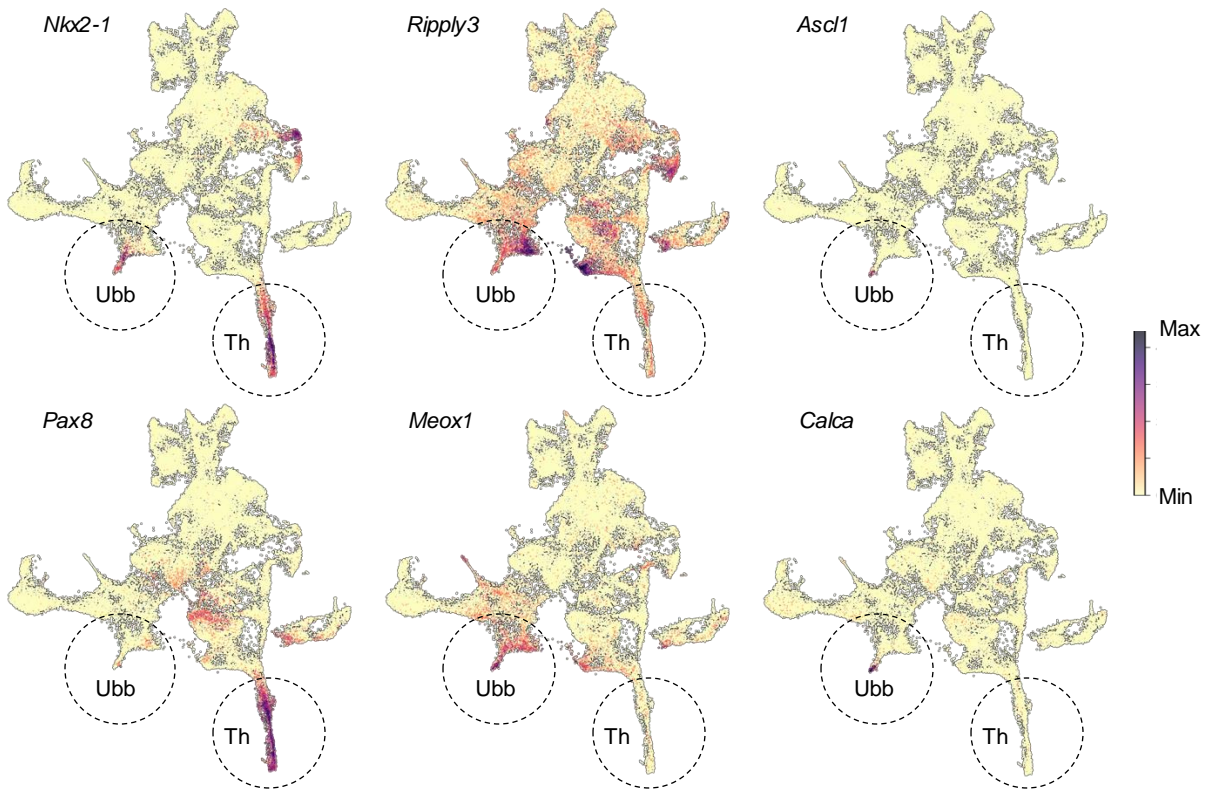


a Pharyngeal endoderm derivatives (E9.5-E12.5)



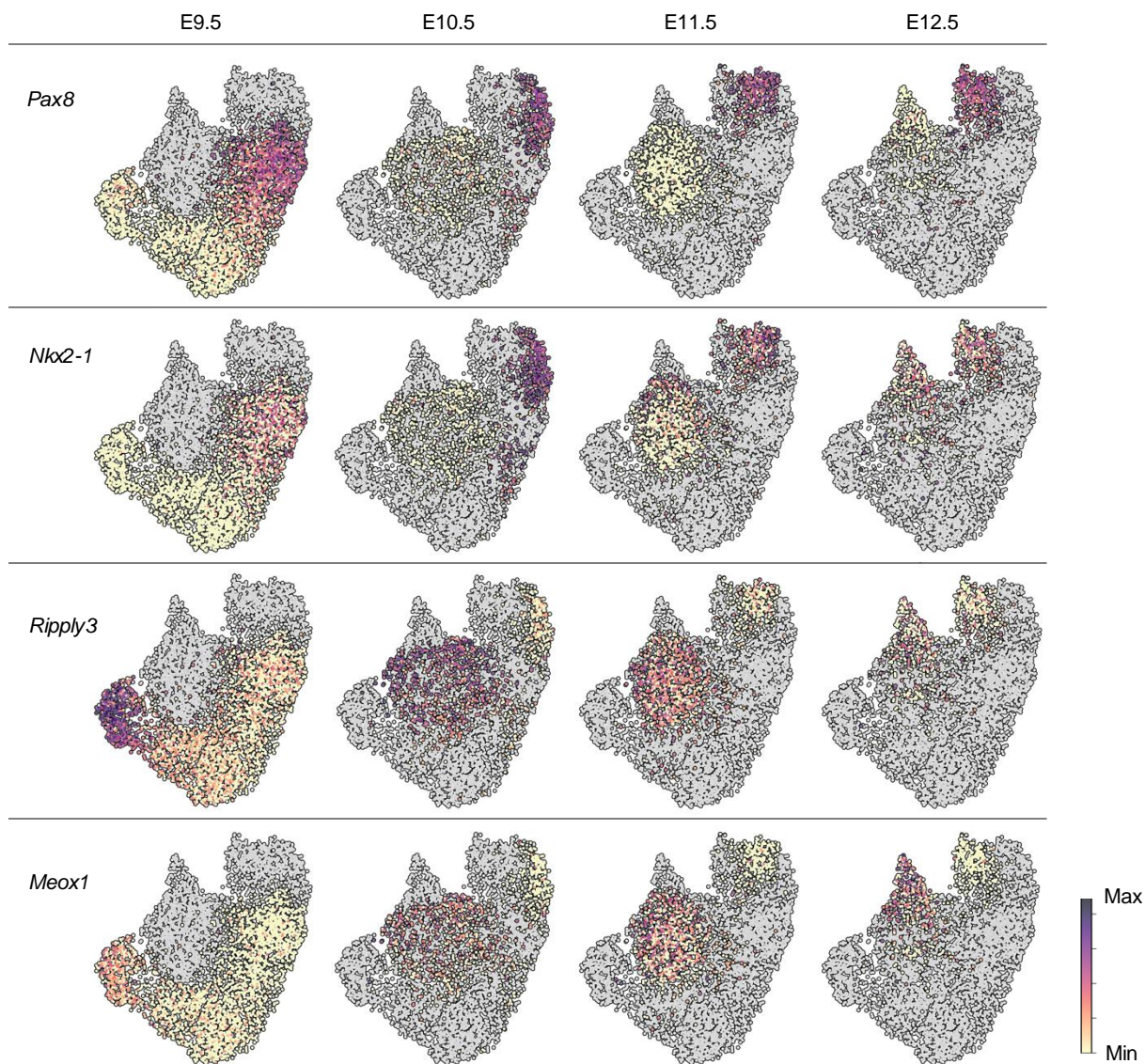
(Modified from:
Magaletta, Lobo, Kernfeld et al, 2022)

b

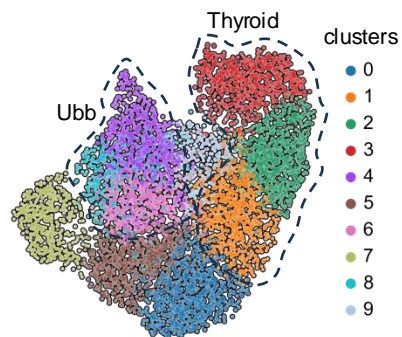


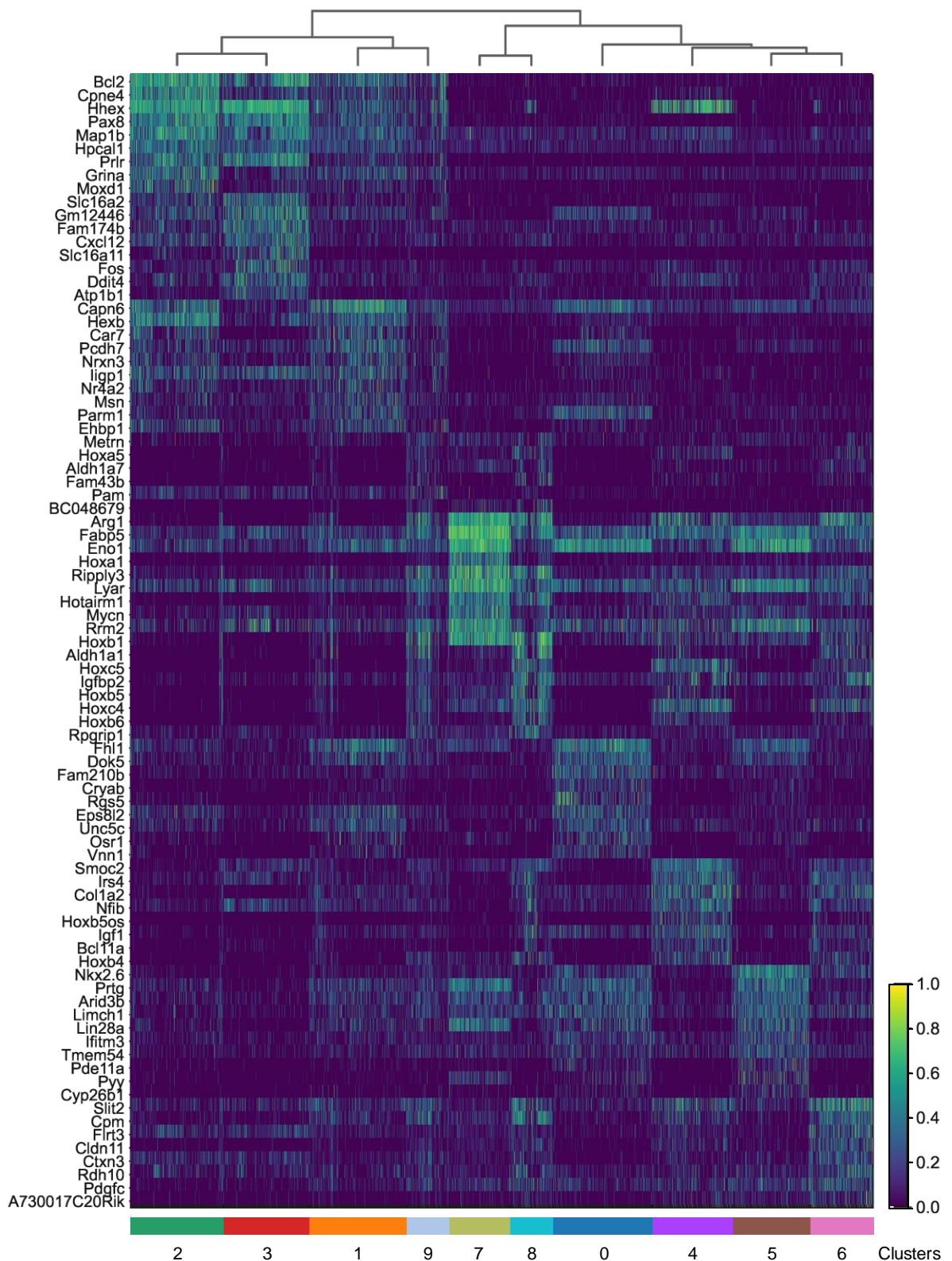
Supplementary Fig. 1. UMAP visualization of select thyroid and ultimobranchial body marker genes.

Extracted from the single-cell transcriptome catalog previously generated from *Pax9*^{VENUS} embryos harvested daily between embryonic days (E)9.5 and E12.5 (Magaletta et al, 2022). **a** Overview depicting unsupervised clustering with the earlier less mature stages being distributed centrally in the UMAP embedding whereas the more mature and organ-specific cells are found in the peripheral clusters, as indicated. **b** Cluster-specific enrichment of the indicated genes of interest. Each dot represents a single cell in the global transcriptome space colored by average log2 normalized expression. Thyroid (Th) and ultimobranchial body (Ubb) clusters are encircled. Scalebar indicates log2-normalized expression.

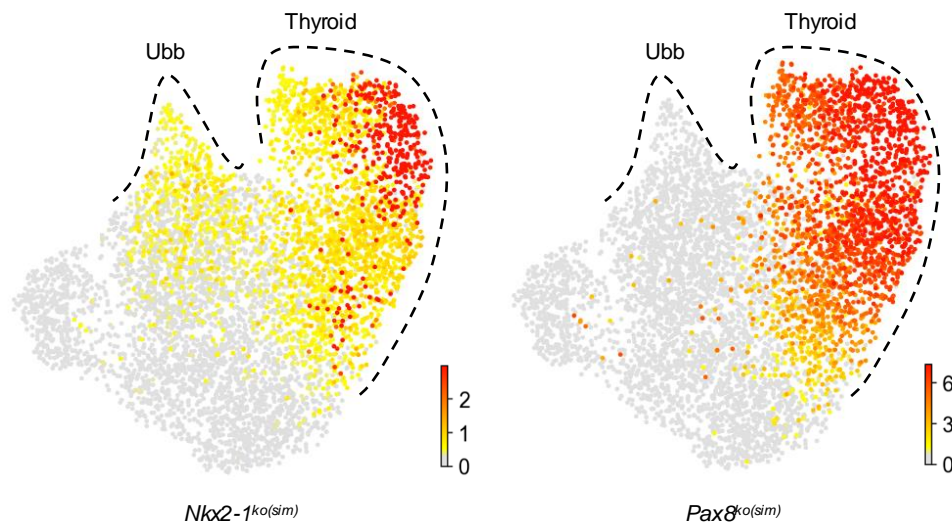


Supplementary Fig. 2. Single-cell mRNA expression of thyroid and ultimobranchial lineage marker genes across Eday. UMAP embedding of differentially expressed *Pax8*, *Nkx2-1*, *Ripply3* and *Meox1* separately shown from each embryonic day between E9.5 and E12.5 (top panels). Cells are outlined and colored by the log2-normalized expression, if they are present at the corresponding embryonic day, and colored gray otherwise. Leiden cluster assignments with thyroid lineage clusters (1-3) and ultimobranchial clusters (4, 6 and 8) encircled, according to unsupervised global scRNAseq analysis, are shown for comparison (right panel). Scalebar indicates log2-normalized expression.

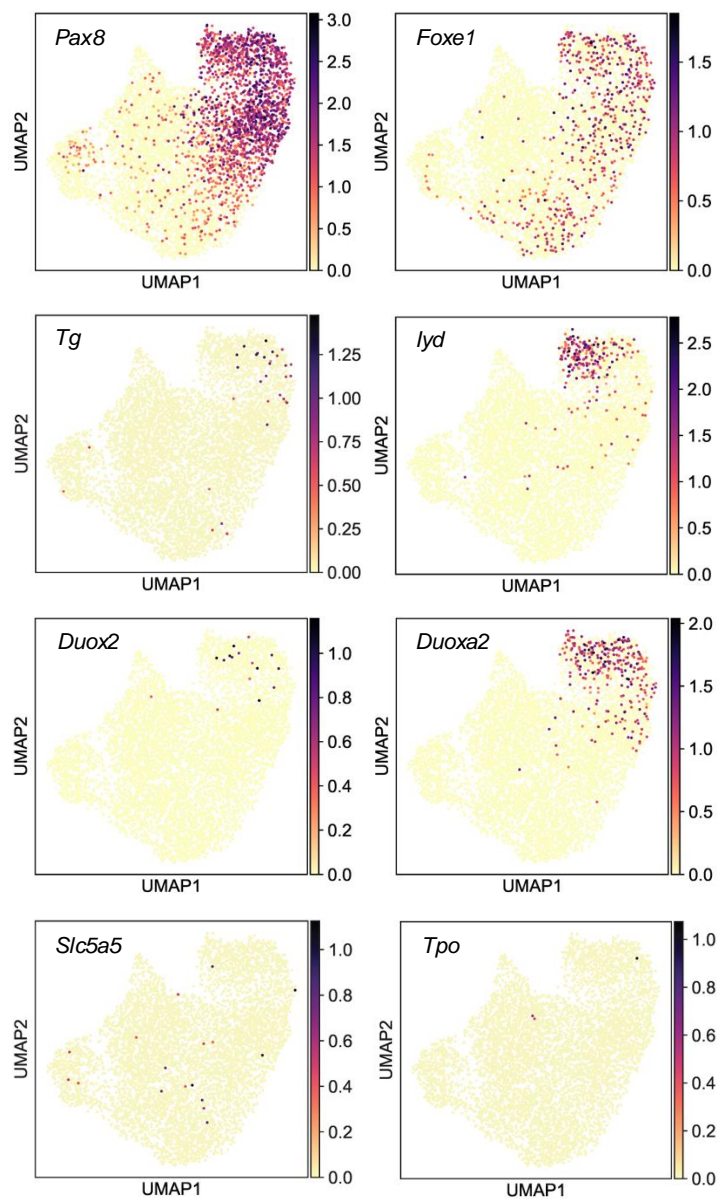




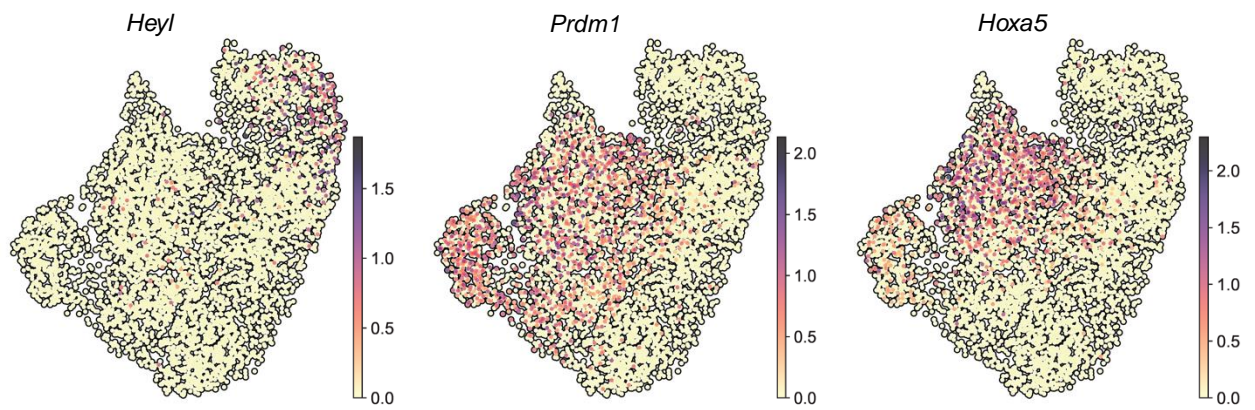
Supplementary Fig. 3. Clusters with thyroid and ultimobranchial lineage identities distinguished by enriched genes. Heatmap showing the scaled expression of the of top 10 upregulated genes in each of clusters 0-9 exclusively featuring an adjusted p-value <0.01, a log2-fold change >1.0, and being expressed in >20% of the cells in the cluster. Genes upregulated in multiple clusters are displayed corresponding to the cluster having maximum average log2-normalized expression of the gene. The dendrogram obtained from unsupervised hierarchical clustering is displayed. Scalebar indicates log2-normalized expression.



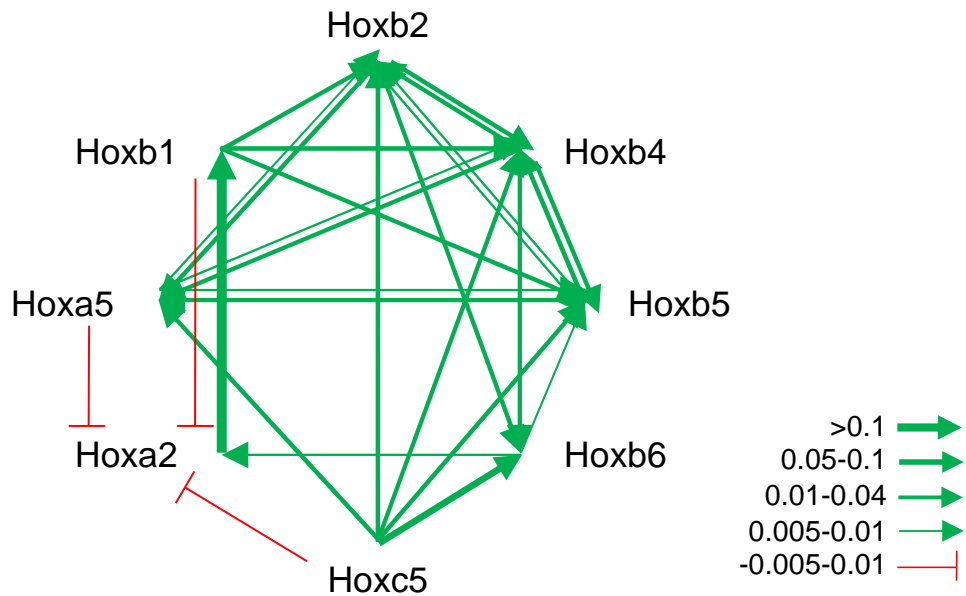
Supplementary Fig. 4. Knockout simulations (ko(sim)) of *Nkx2-1* (left panel) and *Pax8* (right panel) based on GRN inference and predicted cell-state changes with velocity analysis. Both panels show the per-cell magnitude of expression change in the simulated knockout overlaid UMAP embedding of clusters 0-9. Expectedly, ko(sim) of *Nkx2-1* affects both thyroid and ultimobranchial (Ubb) lineage cells whereas ko(sim) of *Pax8* is restricted to cells with thyroid identity. Corresponding visualizations of velocity streams using scVelo are shown in Figs. 5l and m. Bars indicate magnitude of expression change.



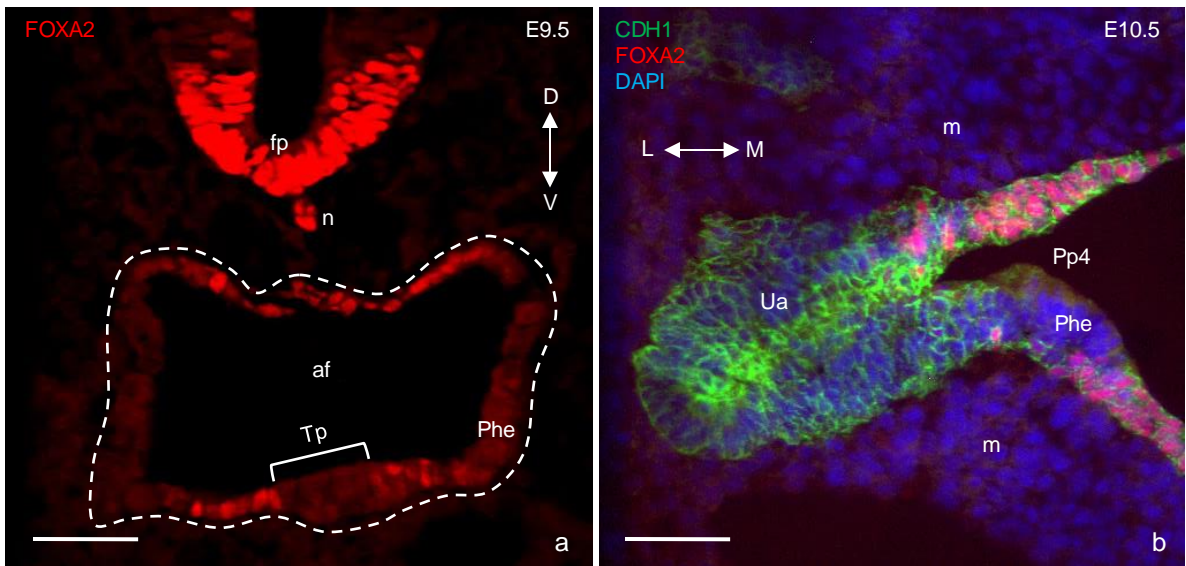
Supplementary Fig. 5. Amounts and distribution of cells expressing thyroid differentiation genes. UMAPs displaying the per cell log2-normalized expression of genes implicated in thyroid differentiation and hormonogenesis obtained from the Gene Ontology database.



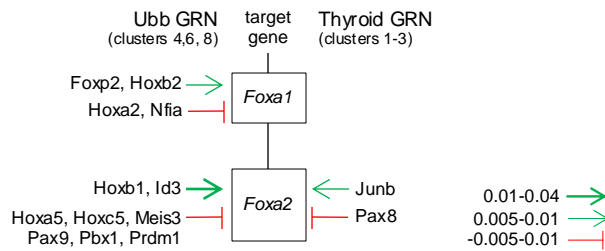
Supplementary Fig. 6. Differential pattern of expression of *Heyl*, *Prdm1* and *Hoxa5* in thyroid and ultimobranchial lineage cells. UMAPs displaying the per cell log2-normalized expression of the indicated genes.



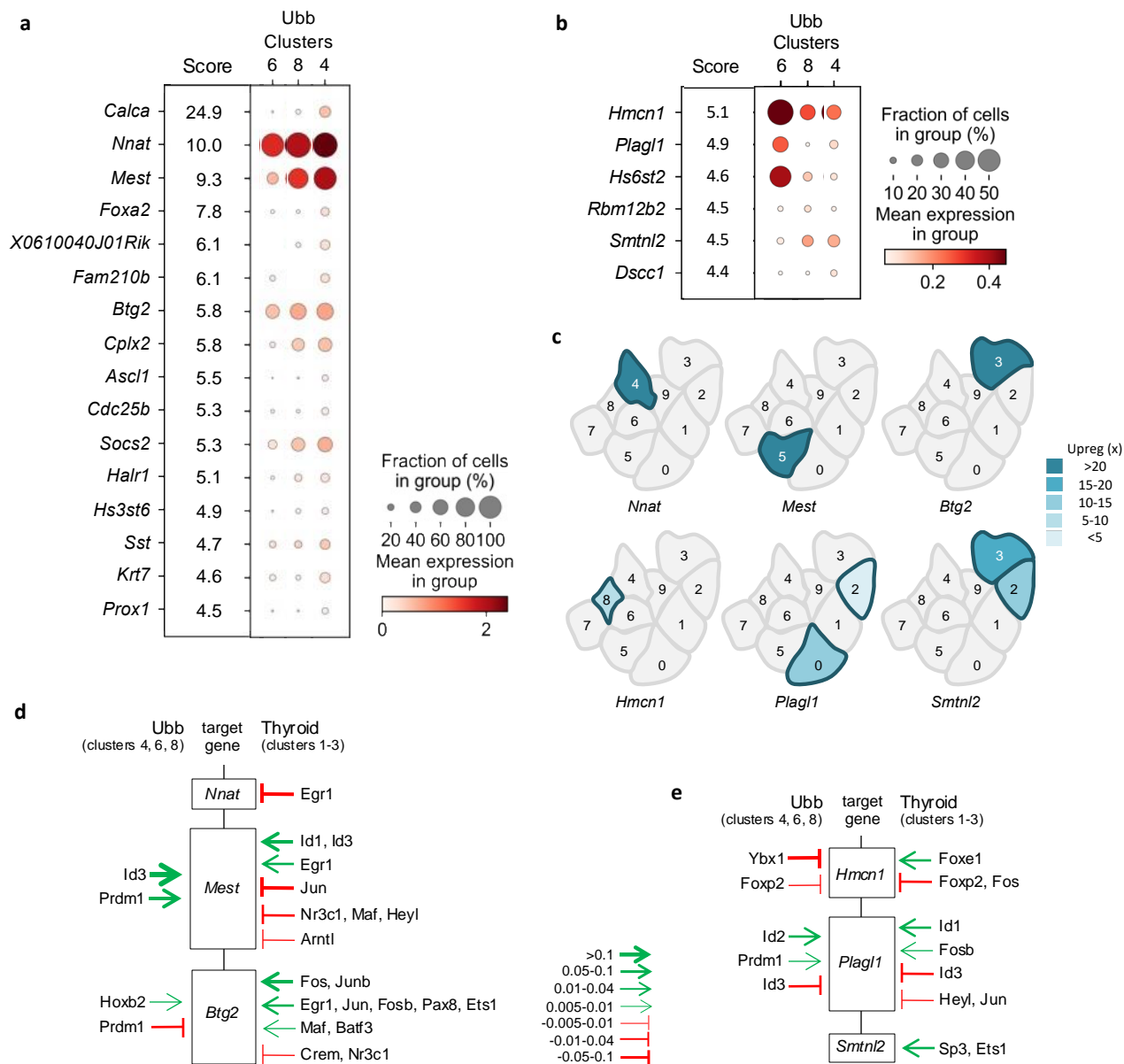
Supplementary Fig. 7. Multiple Hox genes interact in the gene regulatory network of the ultimobranchial lineage. Schematic subnetwork comprising all Hox genes identified by CellOracle predicted to participate in the ultimobranchial body gene regulatory network (Ubb-GRN). Up- versus downregulation are indicated by sharp (green) or blunt (red) arrows and arrow thickness represents mean cluster-specific GRN TF-target gene interaction scores.



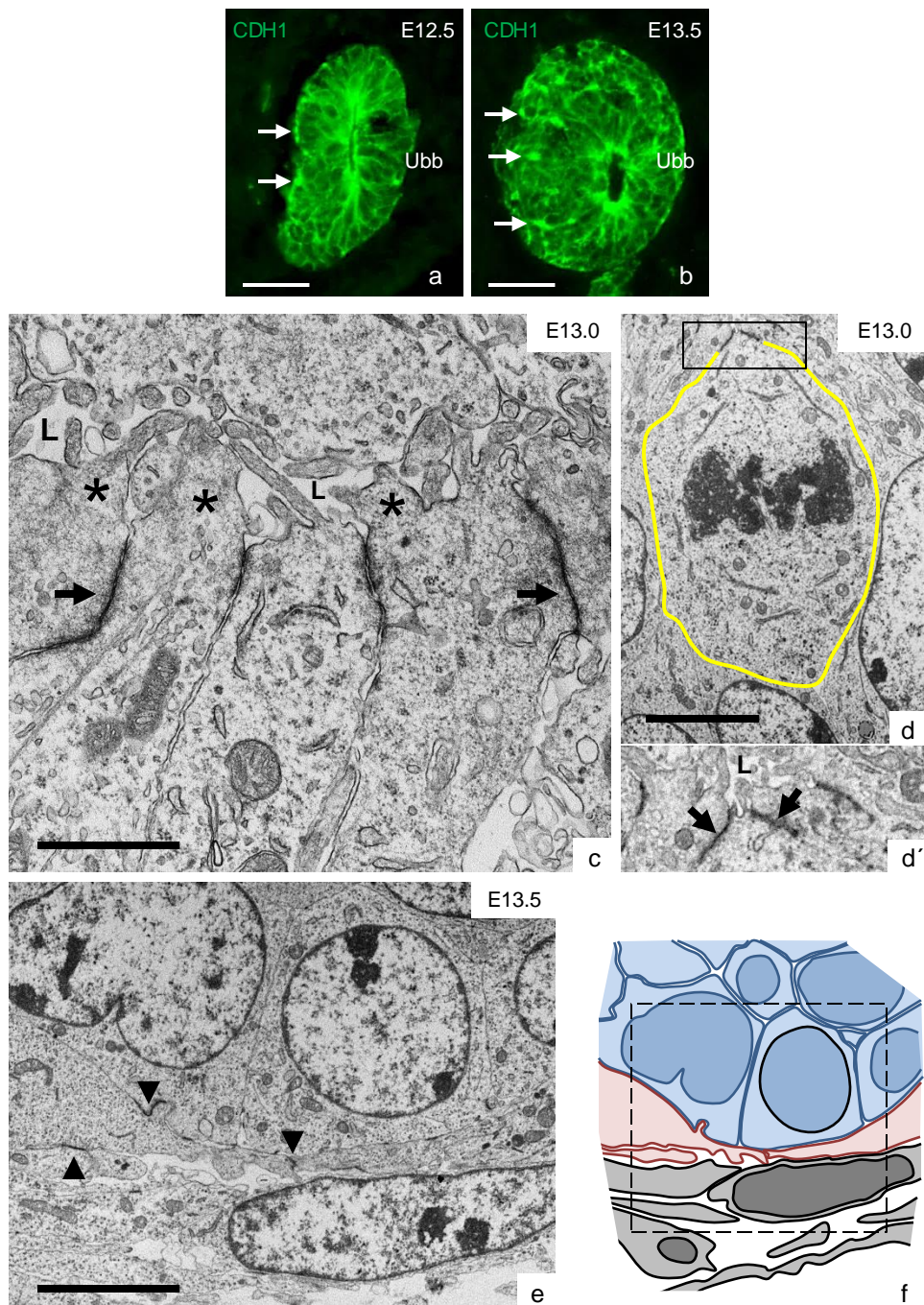
Supplementary Fig. 8. Loss of Foxa2 expression in thyroid and ultimobranchial progenitor cells present in pharyngeal endoderm. **a** Placode stage of thyroid development preceding budding of thyroid primordium from the pharyngeal floor. **b** Prospective ultimobranchial body (Ubb) emerging from pharyngeal pouch endoderm. Immunofluorescence of FOXA2 (single channel in (a) for improved resolution of expression level variations) and E-cadherin (CDH1) with DAPI counterstaining of nuclei. Orientation arrows: D dorsal, V ventral, L lateral, M medial. Phe pharyngeal endoderm, Pp4 fourth pharyngeal pouch, Tp thyroid placode (margins indicated with bracket), Ua Ubb anlage, af anterior foregut (encircled), m mesenchyme, n notochord, fp floor plate. Scale bars: 100 μm (a) and 50 (b) μm .



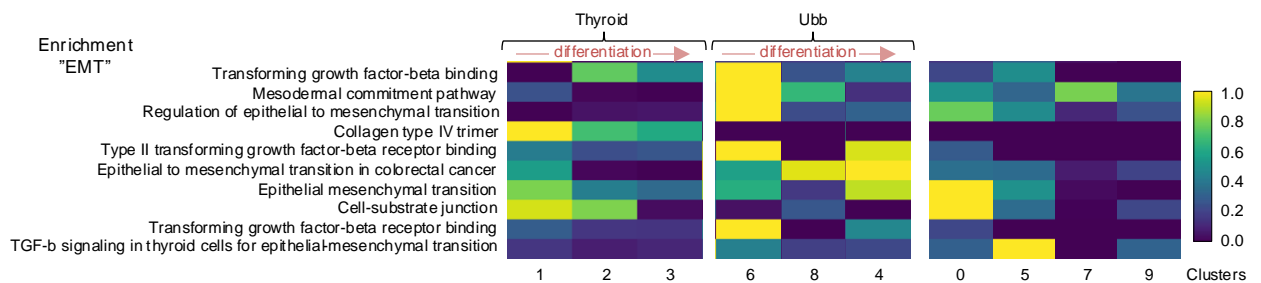
Supplementary Fig. 9. Transcriptional regulation of *Foxa1* and *Foxa2* in Ubb and thyroid GRNs as identified by CellOracle. Predicted up- and downregulation are indicated by sharp (green) or blunt (red) arrows and arrow thickness representing mean cluster-specific GRN TF–target gene interaction scores.



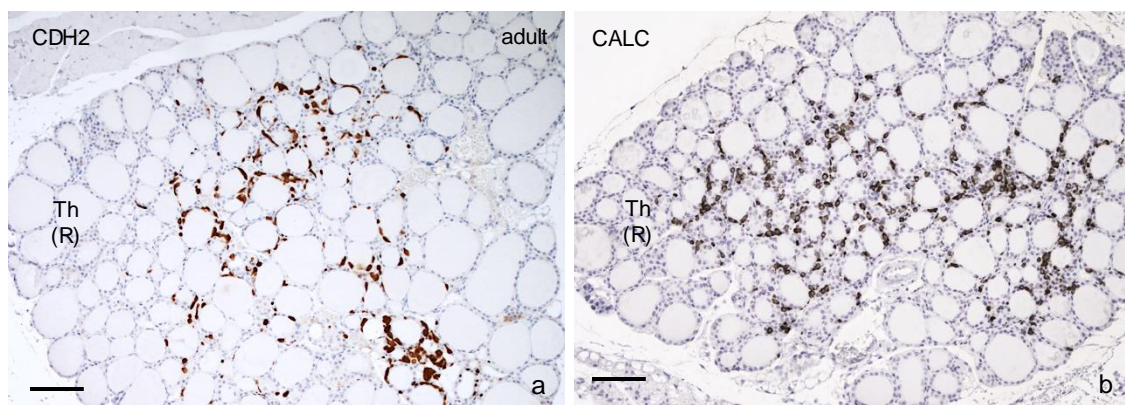
Supplementary Fig. 10. Differential expression and predicted transcriptional regulation of genes enriched in calcitonin positive and calcitonin negative cells of the ultimobranchial lineage. **a, b** Dot plots displaying genes upregulated (adjusted p-value < 0.01, log2-fold change > 1.0) in *Calca* positive cells compared to *Calca* negative cells (a) and *Calca* negative cells compared to *Calca* positive cells (b) of the ultimobranchial body (Ubb). *Calca* positive cells are defined as those having normalized expression of *Calca* > 0 and the Ubb is defined as cells belonging to clusters 4, 6, and 8. The size of the dot indicates the fraction of cells in the cluster expressing the marker, and the color indicates the mean log2-normalized expression of the marker. Scores indicate the z-scores for each gene in the differential comparison between *Calca* positive and negative cells and vice versa. The encoded gene characteristics are shown in Supplementary Table 2a and b. **c** Cluster-specific upregulation of select genes enriched in *Calca* positive (upper panel) and *Calca* negative (lower panel) Ubb cells. Curated from lists comprising all enriched genes per cluster. **d, e** Predicted transcriptional regulation of select genes enriched in *Calca* positive (d) and *Calca* negative (e) cells as identified by CellOracle in the Ubb-GRN. Predicted up- and downregulation are indicated by sharp (green) or blunt (red) arrows and arrow thickness representing mean cluster-specific GRN TF–target gene interaction scores.



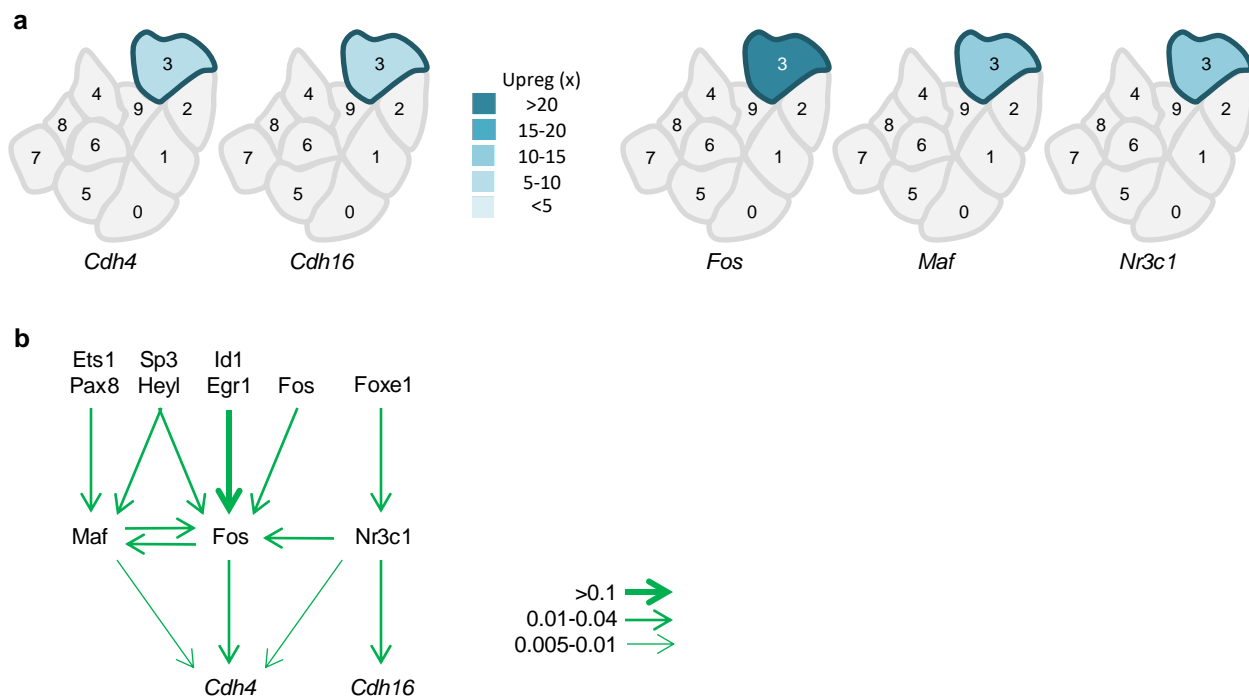
Supplementary Fig. 11. Junctional changes during multilayering of the developing ultimobranchial body epithelium. Immunofluorescence of CDH1 and transmission electron micrographs of the ultimobranchial body (Ubb) between E12.5 and E13.5. **a, b** Appearance of CDH1⁺ focal contacts (arrows). **c** Apical cell changes accompanying constriction of the central lumen (L). Arrows indicate elongated adherens junctions and asterisks mark protrusions of apical cytoplasm. **d** Ubb cell (outlined) undergoing oriented cell division signified by mitotic spindle perpendicular to the apical-basal axis. **d'** Narrowed apical surface of the mitotic cell; high power of boxed area in (d). **e** Basal portions of Ubb partly enclosed by the thyroid primordium. Arrows indicate focal adhesions sites. **f** Reproduced from (e) (framed in drawing), deduced cell identities at the interface of the Ubb perimeter (d), *blue*: Ubb cells; *pink*: follicular progenitors derived from thyroid primordium; *gray*: mesenchymal cells. Scale bars: 5 (b, c) and 2 (a) μm .



Supplementary Fig. 12. Differential expression of genes involved in epithelial-to-mesenchymal transition during thyroid and ultimobranchial lineage development. Heatmap of a curated list of pathways associated with epithelial-mesenchymal transition (EMT) with heat indicating the row normalized $-\log_{10}$ adjusted p-values (Benjamini–Hochberg) obtained from the same enrichment analysis as in Fig. 5e. Cluster panels are grouped for time-dependent comparison of thyroid and ultimobranchial trajectories as indicated. Ontology terms from Gene_Ontology and WikiPathway databases.



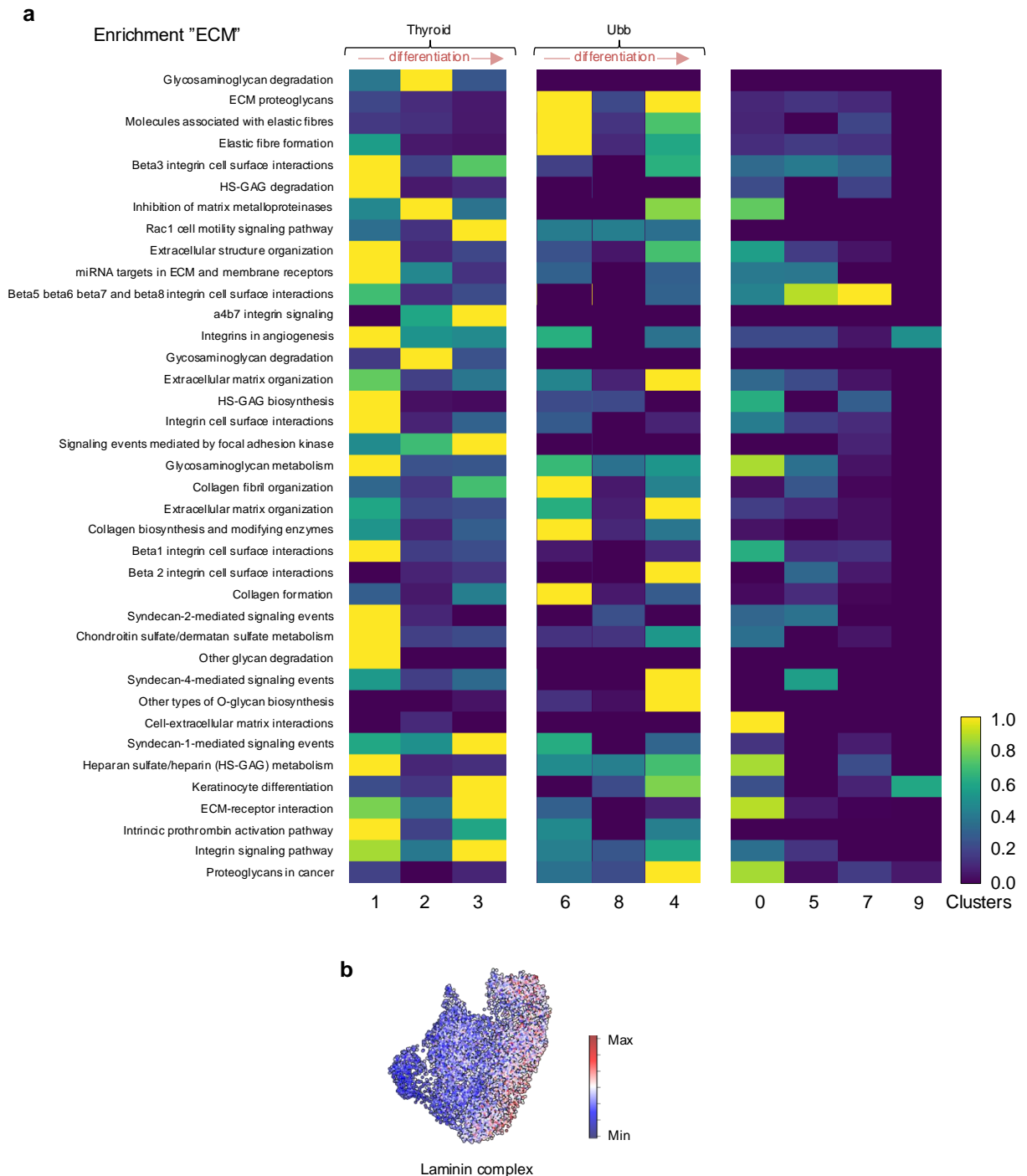
Supplementary Fig. 13. Parafollicular distribution of N-cadherin/Cdh2 positive cells and C-cells in the adult thyroid gland. Immunohistochemical staining of CDH2 (a) and calcitonin (CALC) in paraffin sections of mouse thyroid tissue. Th(R) right thyroid lobe. Scale bars: 100 μ m.



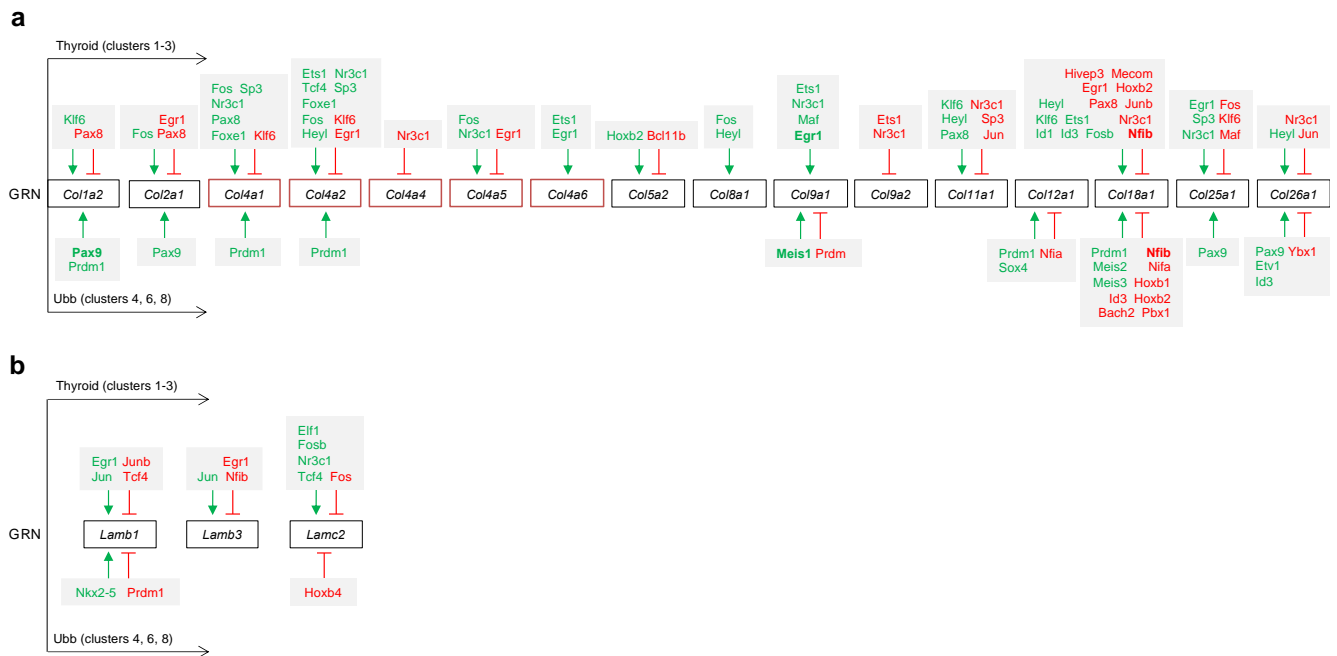
Supplementary Fig. 14. Enriched expression of cadherin-4 (R-cadherin) and cadherin-16 (Ksp-cadherin) and their predicted transcriptional regulators in embryonic thyroid cells undergoing differentiation.

a Cluster-specific upregulation of *Cdh4* and *Cdh16* (left panel) and of transcription factors (TFs, right panel) identified by CellOracle in the thyroid-GRN. Curated from lists comprising all enriched genes per cluster.

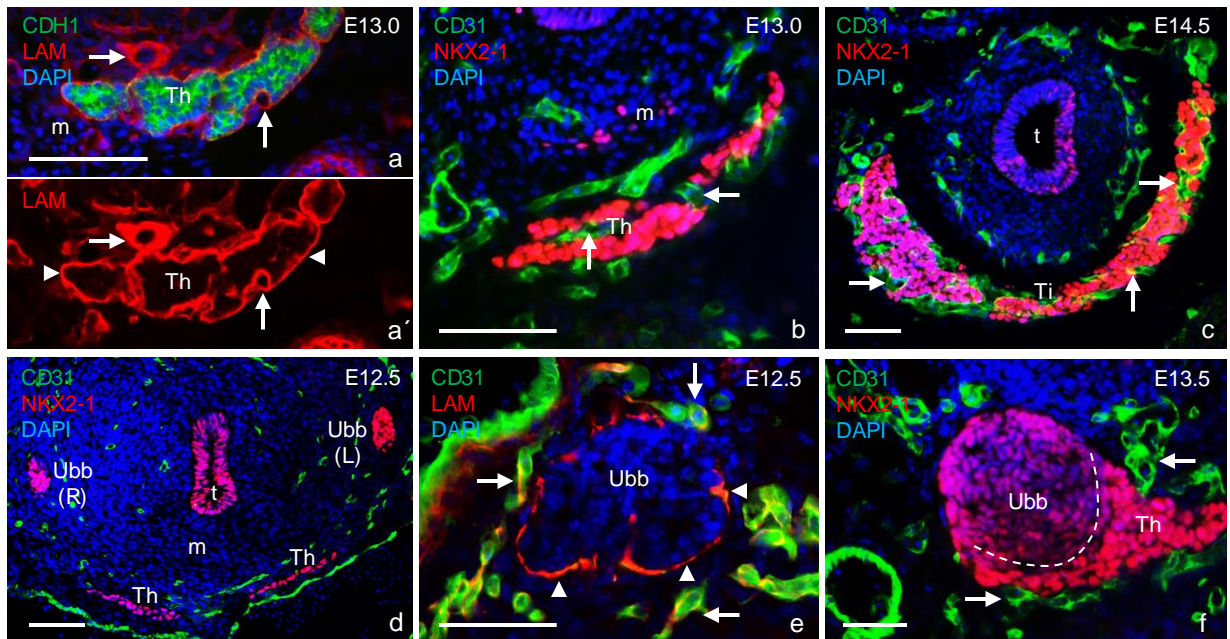
b Predicted subnetwork of *Cdh4* and *Cdh16* regulation in thyroid lineage cells. Arrows indicate upregulation with arrow thickness representing mean cluster-specific GRN TF-target gene interaction scores. No TFs were found to downregulate these cadherins in any single-cell clusters. *Nfia* was predicted to weakly upregulate *Cdh4* in the Ubb-GRN (data not shown).



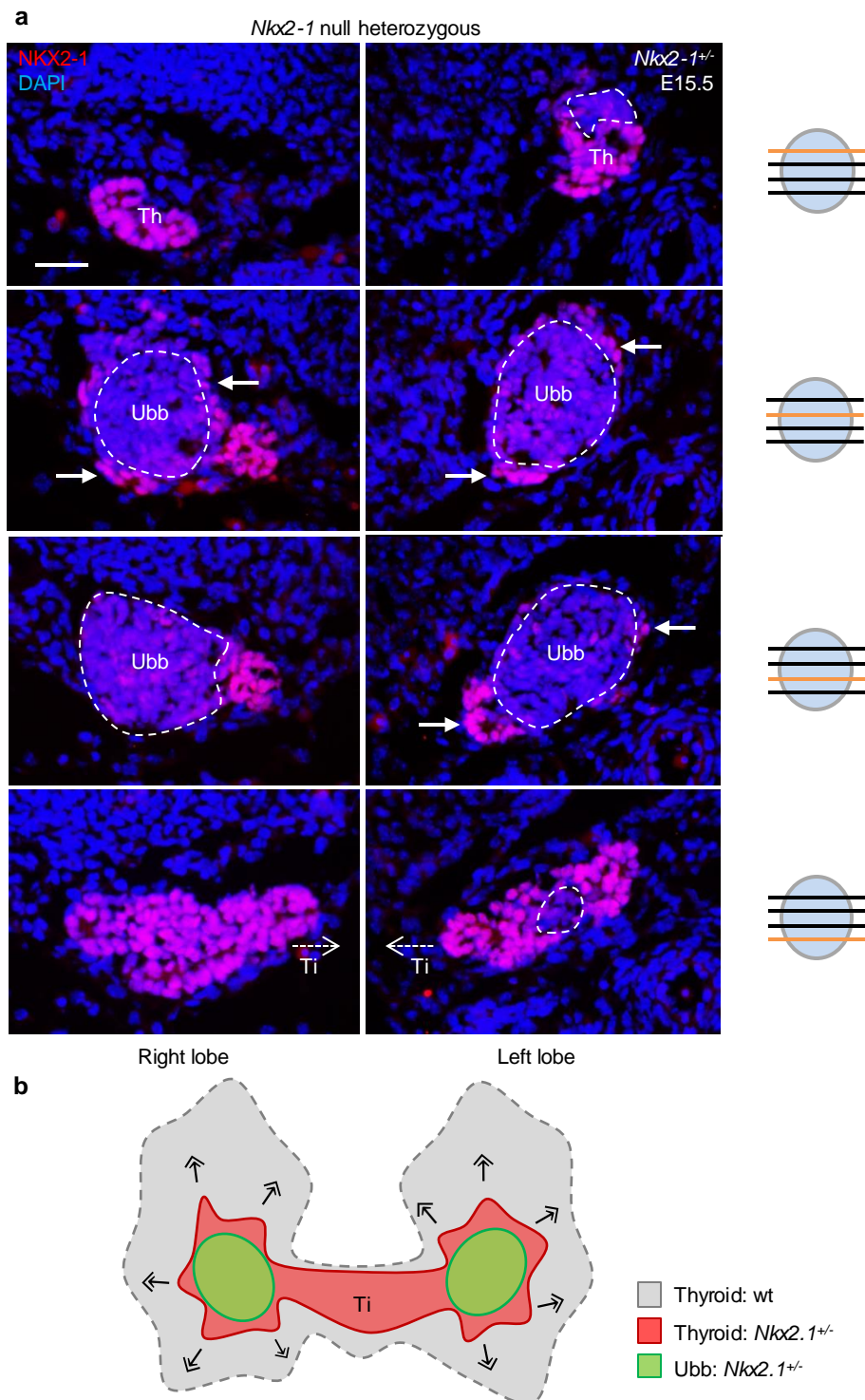
Supplementary Fig. 15. Differential expression of genes involved in turnover and regulation of extracellular matrix constituents during thyroid and ultimobranchial lineage development. **a** Heatmap of a curated list of pathways from Gene Ontology, Reactome and WikiPathway databases associated with extracellular matrix (ECM) with heat indicating the row normalized $-\log_{10}$ adjusted p-values (Benjamini–Hochberg) obtained from an enrichment analysis (with EnrichR) of the genes differentially upregulated (adjusted p-value < 0.01 , \log_2 -fold change > 1.0) in each cluster over a background comprising the remaining clusters. Scale bar indicates scaled $-\log_{10}$ (adjusted value). **b** UMAP displaying the per cell scores of the genes collectively identified in the laminin complex obtained from the Gene Ontology database. Scores are defined as the average \log_2 -normalized expression of the set of genes minus the average \log_2 -normalized expression of a background set. Ubb, ultimobranchial body. Scale bar indicates gene set score.



Supplementary Fig. 16. Inferred regulatory networks of collagen and laminin gene expression differ between thyroid and ultimobranchial cells. **a, b** Schematic subnetworks comprising collagen (*Col*) genes (a) and laminin (*Lam*) genes (b) identified by CellOracle and suggested to be differentially regulated in clusters with thyroid and ultimobranchial lineage identities, respectively. Genes encoding basement membrane-specific collagen type IV alpha-chains are boxed in red. Predicted up- versus downregulation by the indicated transcription factors (TFs) are colored green or red and by corresponding sharp or blunt arrows. Except for Nfib, which is predicted to strongly suppress *Coll8a1* in both lineages, due to space limitation no information is provided on strength of betweenness designating importance of a single TF among others in a given subnetwork. Ubb ultimobranchial body, GRN, gene regulatory network.



Supplementary Fig. 17. Microvessel distribution and associated laminin in the developing thyroid and ultimobranchial bodies. **a-c** Embryonic thyroid vascularization. **d-f** Exclusion of vessels in ultimobranchial epithelial tissues (border towards thyroid outlined in f). Double immunofluorescence of laminin (LAM), CD31, NKX2-1 and CDH1 with DAPI counterstaining of nuclei. Arrows indicate laminin⁺/CD31⁺ vessels. Arrowheads indicate laminin⁺ basal laminae. Th thyroid, Ti thyroid isthmus, Ubb ultimobranchial body, m mesenchyme, t trachea, L left, R right. Scale bars: 100 (c, d) and 50 (a, b, e, f) μm .



Supplementary Fig. 18. Impaired thyroid growth in *Nkx2-1* null heterozygous mouse embryos. **a** Stack of images from serially sectioned thyroid lobe rudiments obtained at E15.5. Cartoons (*left panels*) indicate section levels accounting both rudimentary lobes. Residual NKX2-1^{low} cells of the ultimobranchial body (encircled) are incompletely surrounded by NKX2-1^{high} cells (arrows) derived from the thyroid primordium. Medial direction of isthmus portion is indicated (dashed arrows). Scale bar: 25 μ m. **b** Schematic representation of thyroid (red) and ultimobranchial (green) tissues in *Nkx2-1* null mutant overlaid wildtype (wt, gray) thyroid of same age embryos. Blocked arrows (\rhd) symbolize impaired branching growth of thyroid parenchyma in mutants. Th thyroid, Ubb ultimobranchial body, Ti thyroid isthmus.